# Active Site of Mercuric Reductase Resides at the Subunit Interface and Requires $Cys_{135}$ and $Cys_{140}$ from One Subunit and $Cys_{558}$ and $Cys_{559}$ from the Adjacent Subunit: Evidence from in Vivo and in Vitro Heterodimer Formation†

Mark D. Distefano,‡ Melissa J. Moore,§ and Christopher T. Walsh*

*Department of Biological Chemistry and Molecular Pharmacology, Harvard Medical School, 25 Shattuck Street, Boston, Massachusetts 02115*

*Received August 2, 1989; Revised Manuscript Received October 27, 1989*

ABSTRACT: Mercuric reductase catalyzes the two-electron reduction of Hg(II) to Hg(0) using NADPH as the reductant; this reaction constitutes the molecular basis for detoxification of Hg(II) by bacteria. The enzyme is an $\alpha_2$ homodimer and possesses two pairs of cysteine residues, $Cys_{135}$ and $Cys_{140}$ (redox-active pair) and $Cys_{558}$ and $Cys_{559}$ (C-terminal pair), which are known to be essential for catalysis. In the present study, we have obtained evidence for an intersubunit active site, consisting of a redox-active cysteine pair from one subunit and a C-terminal pair from the adjacent subunit, by reconstituting catalytic activity both in vivo and in vitro starting with two inactive, mutant enzymes, $Ala_{135}Ala_{140}Cys_{558}Cys_{559}$ (AACC) and $Cys_{135}Cys_{140}Ala_{558}Ala_{559}$ (CCAA). Genetic complementation studies were used to show that coexpression of AACC *and* CCAA in the same cell yielded an $Hg^R$ phenotype, some $10^4$-fold more resistant than cells expressing only one mutant. Purification and catalytic characterization of a similarly coexpressed protein mixture showed the mixture to have activity levels ca. 25% those of wild type; this is the same as that statistically anticipated for a CCAA–AACC heterodimeric/homodimeric mixture with only one functional active site per heterodimer. Actual physical evidence for the formation of active mutant heterodimers was obtained by chaotrope-induced subunit interchange of inactive pure CCAA and AACC homodimers in vitro followed by electrophoretic separation of heterodimers from homodimers. Taken together, these data provide compelling evidence that the active site in mercuric reductase resides at the subunit interface and contains cysteine residues originating from separate polypeptide chains.

Mercuric reductase catalyzes the two-electron reduction of mercuric ions to elemental mercury with concomitant oxidation of reduced nicotinamide by the following reaction:

$$Hg(SR)_2 + NADPH + H^+ \rightarrow Hg(0) + NADP^+ + 2RSH$$

This reaction constitutes the last and crucial step in the bacterial mercury detoxification pathway [see Silver and Misra (1988) and Summers (1986) for recent reviews] which includes a specific Hg(II) uptake system (encoded by the *merP* and *merT* genes in the Tn*501 mer* operon) as well as the reductase (encoded by *merA*). Mercuric reductase from several sources exists as an $\alpha_2$ *homodimer* (Fox & Walsh, 1982; Wang et al., 1989). The enzyme also possesses a redox-active disulfide [between $Cys_{135}$ and $Cys_{140}$ in Tn*501*-derived mercuric reductase (Fox & Walsh, 1983)] and an FAD cofactor (Fox & Walsh, 1982), which, along with strong active-site sequence similarity (Fox & Walsh, 1983; Brown et al., 1983), make it a member of the pyridine nucleotide disulfide oxidoreductase family that includes glutathione reductase (Krauth-Siegel et al., 1982), lipoamide dehydrogenase (Stephens et al., 1983), and trypanothione reductase (Shames et al., 1986). Site-directed mutagenesis studies in which the cysteine residues at the 135–140 locus were changed to serine (Schultz et al., 1985) or alanine (Distefano et al., 1989), as well as stopped-flow spectrophotometric experiments (Miller et al., 1986), have conclusively demonstrated that the redox-active cysteines, $Cys_{135}$ and $Cys_{140}$, play an essential role in Hg(II) reduction by mercuric reductase.

Despite the similarities between mercuric reductase and other disulfide oxidoreductases, several important differences exist. A linear alignment of the glutathione reductase primary sequence with that of Tn*501* mercuric reductase demonstrates that while these proteins do exhibit extensive homology, two regions show significant divergence (Brown et al., 1983). One such region encompasses an 85 amino acid N-terminal domain in mercuric reductase which has no counterpart in glutathione reductase. Removal of these residues by partial proteolysis has no effect on the in vitro catalytic rate of mercuric reductase (Fox & Walsh, 1983), and thus their function, if any, remains unresolved [see Moore and Walsh (1989)]. The second region of divergence is found at the C-terminus, where residues from both enzymes have been implicated in catalysis. In mercuric reductase, a pair of cysteines ($Cys_{558}Cys_{559}$ in Tn*501*) located two amino acids from the C-terminus of the enzyme are conserved in all mercuric reductases sequenced to date (Brown et al., 1983; Misra et al., 1985; Griffin et al., 1987; Wang et al., 1989). Cysteine to alanine mutagenesis experiments reported by Moore and Walsh (1989) have demonstrated that removal of these cysteines disrupts normal catalytic reduction of Hg(II). Additional spectroscopic, chemical modification, and protein chemistry studies (Miller et al., 1989) have suggested that these residues are situated in close proximity to the redox-active disulfide ($Cys_{135}Cys_{140}$) and FAD cofactor.

If the C-terminal cysteines play a role in catalysis, it is important to determine how these residues, which are located at the extreme C-terminus of the mercuric reductase polypeptide chain, contribute to the active site. One clue comes from the human glutathione reductase crystal structure (Thieme et al., 1981). Inspection of this dimeric molecule

† This work was supported by NIH Grant GM 21643.

* To whom correspondence should be addressed.

‡ Present address: Department of Chemistry, 164-30, California Institute of Technology, Pasadena, CA 91125.

§ Present address: Center for Cancer Research, E17-529, Massachusetts Institute of Technology, 77 Massachusetts Ave., Cambridge, MA 02139.

0006-2960/90/0429-2703$02.50/0 

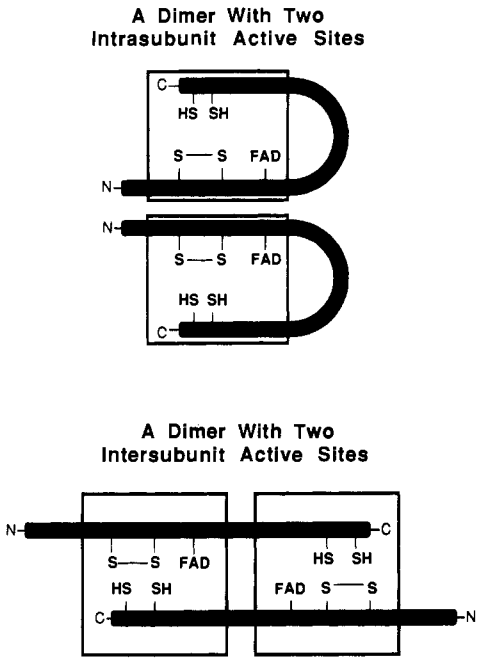


FIGURE 1: Possible intrasubunit and intersubunit active-site arrangements for mercuric reductase. Each active site, which is thought to be composed of both a redox-active disulfide and a C-terminal cysteine pair, together with one FAD cofactor, is boxed. Each intrasubunit active site contains cysteine residues from only a single polypeptide chain while an intersubunit active site requires participation of residues from both subunits. Note that in both cases, there are two active sites per dimer.

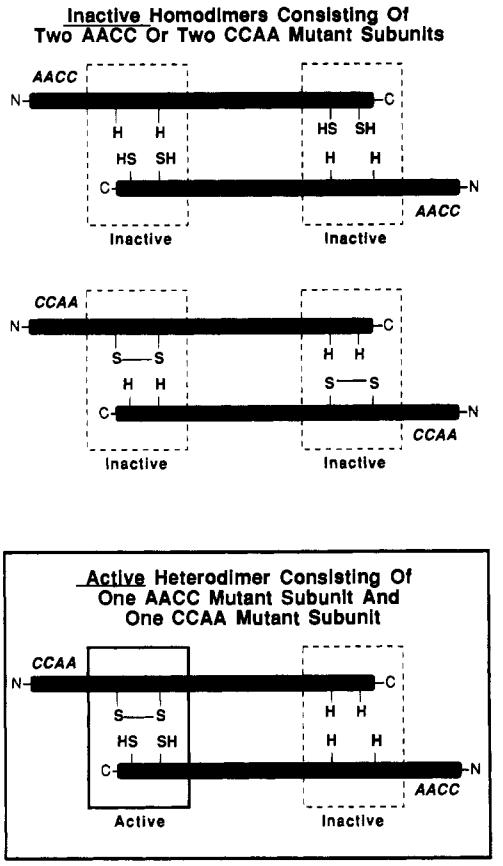


FIGURE 2: Schematic of inactive mutant homodimers and active mutant heterodimers having intersubunit active sites. (Top) Inactive homodimers each composed of two subunits each of the inactive mutants, AACC and CCAA. (Bottom, in box) Active heterodimer consisting of one AACC mutant subunit and one CCAA mutant subunit. The type of mutation (AACC or CCAA) for each subunit is indicated above or below its N-terminus.

indicates that the enzyme active site is comprised not only of residues surrounding the redox-active disulfide and FAD cofactor but also of a crucial histidine originating from the C-terminus of the protein. Further inspection reveals that the key histidine residue is donated from a subunit distinct from that which provides the redox-active disulfide and flavin moieties. Thus, two important points emerge. First, the active site is made up of residues from both subunits and is therefore an intersubunit active site. Second, the histidine residue important for catalysis originates near the C-terminus of the protein *analogous to the location of the C-terminal cysteine pair in mercuric reductase.*

In light of these observations, it is pertinent to ask whether the active site of mercuric reductase is comparably disposed, utilizing a redox-active disulfide from one subunit and a C-terminal cysteine pair from the other subunit, i.e., an intersubunit active site. Alternatively, the active site could be intrasubunit in nature, consisting of C-terminal and redox-active cysteine residues from the same polypeptide chain. Both of these possibilities are schematically illustrated in Figure 1.

In this paper, we report a series of experiments designed to probe the disposition of cysteine residues in the active site of mercuric reductase. These studies involve the in vivo and in vitro production of heterodimeric mercuric reductases generated from inactive bis(alanine), bis(cysteine) [$Ala_{135}Ala_{140}Cys_{558}Cys_{559}$ (AACC)[1] and $Cys_{135}Cys_{140}$-$Ala_{558}Ala_{559}$ (CCAA)] mutant enzymes. If the active site of mercuric reductase is intersubunit in nature, heterodimers produced by reassortment of the inactive AACC and CCAA mutants should contain intact active sites, resulting in a partial restoration of enzyme activity (Figure 2). If, however, the active site is intrasubunit in nature, such heterodimers would remain inactive as no viable active sites would be formed.

The procedures used here to generate heterodimers derive from several important literature precedents. Pioneering work by Fincham and Coddington (1963) with glutamate dehydrogenase and Schlesinger and Levinthal (1963) with alkaline phosphatase demonstrated that the mixing of different inactive mutant enzyme species in vitro could result in active hybrid proteins [see Hatefi and Hanstein (1974) and Jaenicke and Rudolf (1986) for a survey of methods]. In vivo complementation was also demonstrated with alkaline phosphatase by Garen and Garen (1963), who constructed *Escherichia coli* heterozygotes from chromosomal mutants and provided the second gene in trans on an F′ episome. The first example of in vitro heterodimer generation with mutants produced by site-directed mutagenesis was described by Wente and Schachman (1987). In our experiments, heterodimers were first produced in vivo, using a two-plasmid coexpression system. Such a system has been previously reported by Larimer et al. (1987) and was used in the study of ribulose-bisphosphate carboxylase. The present paper extends this methodology in that it allows the results of heterodimer formation to be evaluated directly in vivo by capitalizing on the quantifiable effect on phenotype that a functional mercuric reductase confers upon bacteria challenged with Hg(II).

[1] Abbreviations: AACC, $Ala_{135}Ala_{140}Cys_{558}Cys_{559}$ MerA; amp, ampicillin; CAAA, $Cys_{135}Ala_{140}Ala_{558}Ala_{559}$ MerA; CACC, $Cys_{135}Ala_{140}Cys_{558}Cys_{559}$ MerA; CCAA, $Cys_{135}Cys_{140}Ala_{558}Ala_{559}$ MerA; EDTA, ethylenediaminetetraacetic acid; EOP, efficiency of plating; FAD, flavin adenine dinucleotide; IPTG, isopropyl β-D-thiogalactopyranoside; kDa, kilodalton(s); LB, Luria–Bertani media; $NADP^+$, oxidized β-nicotinamide adenine dinucleotide phosphate; NADPH, reduced β-nicotinamide adenine dinucleotide phosphate; PAGE, polyacrylamide gel electrophoresis; SDS, sodium dodecyl sulfate; thio$NADP^+$, thionicotinamide adenine dinucleotide phosphate.

## Experimental Procedures

### Materials

Restriction enzymes were obtained from New England Biolabs, Bethesda Research Laboratories, or Boehringer Mannheim. T4 DNA ligase, *E. coli* JM109, and kinased *Pst*I linkers were obtained from New England Biolabs. The 1496 bp kanamycin resistance GenBlock was from Pharmacia. Plasmid pGP1-4 (carrying $Kan^R$ and the P15A origin) was a generous gift from Dr. Stanley Tabor, Harvard Medical School, Boston, MA. Plasmid pJOE114 (Brown et al., 1983) was a generous gift from Dr. Nigel Brown, Department of Biochemistry, University of Bristol, Bristol BS8 1TD, U.K. Plasmids pMMa558a559, pMMOa558a559 (Moore & Walsh, 1989), pMDM1, pMDO3 (Distefano et al., 1989), and pPS01, and *E. coli* strain W3110 *lacI*$^q$ (Schultz et al., 1985) were described previously.

### Methods

*DNA Methods.* Routine DNA manipulations were performed as described by Maniatis et al. (1982).

*Construction of pMDO3Kan3.* Plasmid pMDO3 (Distefano et al., 1989) was linearized with *Sca*I, ligated to *Pst*I linkers, and then exhaustively digested with *Pst*I. A Pharmacia GenBlock containing the $Kan^R$ was also digested with *Pst*I. The two fragments were then purified by agarose electrophoresis and ligated together by using T4 DNA ligase, and the ligation mixture was used to transform *E. coli* JM109. Plasmid DNAs isolated from kanamycin-resistant clones were screened for insert by restriction mapping with *Eco*RI and *Hin*dIII. The resultant plasmid, which encodes the AACC mutant *merA* and resistance to kanamycin, but lacks ampicillin resistance due to interruption of *ampC*, was denoted pMDO3Kan3.

*Construction of pMDO3P15A.* Plasmids pMDO3Kan3 and pGP1-4 were each digested with *Bam*HI and *Pst*I and then ligated together without fragment purification. This ligation mixture was used to transform *E. coli* JM109, and plasmid DNA from kanamycin-resistant clones was analyzed by restriction mapping with *Eco*RI, *Hin*dIII, and *Pst*I/*Bam*HI double digestion. The finished construct, carrying the AACC mutant *merA* gene, the kanamycin resistance gene, and the P15A bacterial origin of replication, was denoted pMDO3P15A.

*Efficiency of Plating Assays.* Overnight cultures of *E. coli* JM109 carrying the desired plasmid(s) were grown in LB media supplemented with the appropriate antibiotic(s). These cultures were serially diluted $10^1$–$10^{10}$-fold, and 200 μL from each dilution was spread onto LB plates containing antibiotic(s), antibiotic(s) plus $HgCl_2$, or antibiotic(s) plus $HgCl_2$ and IPTG. Each sample was plated in duplicate, and the plates were incubated at 37 °C for 12–18 h before being scored for growth of colonies. The antibiotic (ampicillin and/or kanamycin) and IPTG concentrations used were 50 μg/mL and 2 mM, respectively. For assays of JM109 alone, plates contained no antibiotics. A total of three $HgCl_2$ concentrations (10, 20, and 50 μM) were tested. The efficiency of plating at each $HgCl_2$ concentration was taken to be the ratio of the number of cells surviving at that $HgCl_2$ concentration to the total number of viable cells (i.e., the number of colonies on the plates containing only antibiotics) (Ni'Bhriain et al., 1983; Ross et al., 1989). The effect of IPTG was determined similarly. By counting the number of $HgCl_2$-surviving colonies on plates derived from low dilutions, but determining the viable cell count from the high-dilution plates, very low efficiency of plating values (ca. $10^{-6}$) can be detected.

*Protein Purification and Quantitation.* Protein purifications were performed as previously described by Schultz et al. (1985). Protein concentrations were estimated by the method of Lowry (1951) or Bradford (1976) using purified wild-type mercuric reductase as a standard. For spectral experiments, protein concentrations were determined from the enzyme-bound FAD extinction coefficients which were previously reported by Fox and Walsh (1982) (wild type), Distefano et al. (1989) (AACC), and Moore and Walsh (1989) (CCAA).

*Aerobic Mercuric Reductase and Transhydrogenation Assays.* These assays were performed as previously described by Fox and Walsh (1982) and Schultz et al. (1985). One unit of enzyme activity is defined as the amount of enzyme that catalyzes the thio-$NADP^+$- or Hg(II)-dependent oxidation of 1 μmol of NADPH per minute.

*Anaerobic Mercuric Reductase Assays.* This assay is a modification of the standard mercuric reductase assay described by Fox and Walsh (1982). Cysteine was used in this assay in place of β-mercaptoethanol since the latter is volatile and subject to evaporation during the degassing procedure. Since Hg(II) is known to stimulate the rate of $O_2$-dependent NADPH consumption by the CCAA mutant, assays were performed anaerobically to eliminate any ambiguity due to this problem. In these assays, 3-mL aliquots of a buffer containing 80 mM sodium phosphate, pH 7.5, 1 mM cysteine, and 200 μM NADPH were added to 13 mm × 100 mm borosilicate glass test tubes fitted with soft rubber stoppers (Green Rubber Co.). These tubes were degassed by using a gas train similar to that described by Beinert et al. (1978) by cycling between vacuum (30 s) and 1.2 atm of argon gas (1–5 min) for a total of 10 cycles. Enzyme and $HgCl_2$ solutions were degassed similarly. An aliquot of enzyme was then transferred to a tube containing degassed assay buffer via a gas-tight syringe, and the background NADPH oxidation rate due to any residual $O_2$ reduction was determined by monitoring the loss of absorbance at 340 nm [$\epsilon_{NADPH}(340\text{ nm}) = 6.2\text{ mM}^{-1}\text{ cm}^{-1}$]. Absorbance measurements were made by using a Hewlett Packard 8452A spectrophotometer thermostated to 37 °C. $HgCl_2$ was then added to each assay tube to a final concentration of 100 μM and absorbance monitoring continued. The rate of Hg(II) reduction was computed by subtracting the background rate of NADPH consumption from that observed in the presence of $HgCl_2$. The protein concentrations used to calculate specific activities were determined by using the enzyme-bound FAD extinction coefficients described above. For the heterodimeric enzyme mixture, the extinction coefficient of the wild-type enzyme was used.

*Scanning Densitometry of Plasmid DNAs Isolated from E. coli JM109 (pMDO3P15A/pMMOa558a559).* The following technique was used to determine the relative ratio of the two plasmids present in *E. coli* JM109 (pMDO3P15A/pMMOa558a559). Plasmid DNA was isolated by the alkaline lysis method (Maniatis et al., 1982), *Eco*RI/*Hin*dIII-digested, and then electrophoresed on a 1% agarose gel containing 1.0 μg/mL ethidium bromide. A Polaroid negative of the gel was scanned by using an LKB scanning densitometer, and the integrated peak areas were determined by weighing peaks cut from an enlarged Xerox copy of the printout. The molecular masses of the pMDO3P15A and pMMOa558a559 fragments were determined from separate digests by comparison of their mobilities upon agarose electrophoresis with those of known standards (*Bst*EII-digested λ DNA). To calculate the relative amount of pMDO3P15A versus pMMOa558a559 present in JM109 (pMDO3P15A/pMMOa558a559) cells, the integrated peak areas described above were normalized by dividing the

peak area for each fragment by its estimated molecular mass. Assuming that the relative ethidium bromide staining intensity of a fragment is linearly proportional to its molecular mass, the relative ratio of pMDO3P15A to pMMOa558a559 could then be calculated from the normalized peak areas.

*Spectral Quantitation Analysis of Heterodimeric Mercuric Reductase.* The quantities of the AACC and CCAA mutant proteins within a sample of heterodimeric mercuric reductase purified from JM109 (pMDO3P15A/pMMOa558a559) were estimated by fitting the visible absorbance spectrum of the heterodimeric mixture to a linear combination of the individual purified AACC and CCAA spectra. This was accomplished by using the Quantitation II software package of a Hewlett Packard 8452A spectrophotometer equipped with a 89500 Hewlett Packard ChemStation. This package utilizes a weighted linear least-squares analysis algorithm to fit the spectrum of an unknown (the heterodimeric protein in this case) to a summation of two known spectra (Hewlett Packard, 1987).

*Exhaustive Dialysis Screen of Chaotropic Agents.* Individually purified wild-type, CCAA, and AACC proteins that had been stored at −70 °C in 15% glycerol were thawed and diluted to approximately 95 μM in purification buffer [20 mM sodium phosphate (pH 7.5), 0.5 mM EDTA, and 0.1% β-mercaptoethanol]. Equimolar amounts of CCAA and AACC were combined to create four 270-μL samples. Each sample was placed in a microdialysis cup and dialyzed against 1.5 M KSCN, 1.5 M $NaClO_4$, or 1.0 M guanidine hydrochloride (all dissolved in purification buffer) or buffer alone. Four 110-μL samples of wild type were similarly treated. After 120 h at 4 °C, samples were removed, treated with excess FAD, and then desalted by gel filtration on Pharmacia NAP-5 columns that had been preequilibrated with purification buffer; 5–10 μL of each desalted sample was assayed (aerobically) for mercuric reductase activity in 100 μM $HgCl_2$, 2 mM β-mercaptoethanol, 200 μM NADPH, and 50 mM potassium phosphate (pH 7.3) at 37 °C. Protein concentrations were determined by using Bradford (1976) assays, and specific activities (after normalizing for protein concentration) were expressed as a percentage of the activity exhibited by wild-type enzyme that had been dialyzed against buffer alone.

*Subunit Interchange vs Time and Chaotrope Concentration.* To determine the time required for complete subunit interchange, three 400-μL samples containing 10 μM AACC, 10 μM CCAA, 30 mM cysteine, 50 μM FAD, 20 mM sodium phosphate (pH 7.5), and 0.5 mM EDTA were prepared and incubated on ice. Two of the samples also contained either 1.5 M KSCN or 1.5 M guanidine hydrochloride. After chaotrope addition, 10-μL aliquots were removed at 15-min time intervals and assayed for mercuric reductase activity as above. To determine the optimal KSCN concentration, samples were made up similarly except that [KSCN] was varied from 0.0 to 1.5 M in 0.1 M steps. After incubation on ice for 2 h, 10-μL aliquots were assayed aerobically as described above.

*Analytical Nondenaturing Gel Electrophoresis of Heterodimeric Mercuric Reductase.* A sample of largely "unclipped" CCAA was prepared by purification from W3110 *lacI*$^q$ (pMMOa558a559) cells (Moore & Walsh, 1989) in the presence of 0.75 mM PMSF. [A control experiment showed that PMSF does not affect the activity of wild-type mercuric reductase (data not shown).] A sample of completely "clipped" AACC, purified from W3110 *lacI*$^q$ (pMD03) cells, was prepared by partial digestion with chymotrypsin followed by affinity chromatography as described in Fox and Walsh (1983). A heterodimeric mixture of these two proteins was prepared by combining equimolar amounts of each (final concentration of 20 μM each) in 20 mM sodium phosphate, pH 7.5, buffer containing 1.5 M KSCN, 30 mM cysteine, 0.5 mM EDTA, and 50 μM FAD. After 3 h of incubation at 25 °C, the sample was desalted into 20 mM sodium phosphate, pH 7.5, buffer using a Pharmacia NAP-10 column. Thirty micrograms of this material was combined with a 2× loading buffer containing 20 mM sodium phosphate, pH 7.5, 10% glycerol (v/v), and 0.002% bromphenol blue (w/v) and loaded onto a nondenaturing discontinuous 10% polyacrylamide gel using a high-pH buffer system (stacks at pH 8.3, separates at pH 9.5) described by Davis (1964). Following electrophoretic separation at 4 °C, protein bands were visualized by staining with Coomassie blue.

*Preparative Nondenaturing Gel Electrophoresis, Elution, and Activity Measurement of Heterodimeric Mercuric Reductase Prepared in Vitro.* A heterodimeric mixture of AACC/CCAA mercuric reductases was prepared and electrophoresed as above on a preparative thickness (3 mm) gel. Following electrophoresis, the two end lanes (30 μg of protein each) were removed with a razor blade, Coomassie stained and destained for 1 h each, and then incubated in electrophoresis buffer for an additional 30 min. This latter step was necessary to shrink the gel strips back to as near their original sizes as possible (the gel expands in the stain and destain solutions). These gel strips were then placed alongside the unstained portion of the gel (which had been stored at 4 °C during the staining and destaining of the end lanes) where they were used as guides in locating the protein bands on the unstained gel (240 μg of protein total). Horizontal gel slices containing each band were excised and eluted from the gel by shaking each slice in a 15-mL polyethylene tube containing 5 mL of 20 mM sodium phosphate, pH 7.5, 0.5 mM EDTA, 0.1% β-mercaptoethanol, and 1 mM PMSF for 8 h at 4 °C. Following elution, the samples were concentrated by ultrafiltration (Amicon PM30) to a final volume of ca. 50 μL and analyzed by SDS–PAGE.

## Results

*Evidence for Heterodimeric Mercuric Reductase Formation in Vivo: E. coli Expressing both AACC and CCAA Mutant Mercuric Reductases Show Enhanced $HgCl_2$ Resistance Levels.* As a first test of the hypothesis that the active site of mercuric reductase contains cysteine residues from the redox-active disulfide ($Cys_{135}Cys_{140}$) of one subunit and the C-terminal cysteine pair ($Cys_{558}Cys_{559}$) of the other subunit in each enzyme dimer, we chose to employ the method of genetic complementation. Specifically, we have examined the ability of a double mutation in the redox-active disulfide (AACC) to complement in trans a double mutation in the C-terminal cysteine pair (CCAA). The AACC mutant was also tested for complementarity to other redox-active disulfide mutants. Complementation analysis was done by simply comparing the levels of resistance to mercuric ions exhibited by cells expressing the mutant proteins alone or in combination. Since mercuric ion resistance levels are highly dependent on the functional state of mercuric reductase (vide infra), such phenotypic analysis could provide immediate information as to the validity of our structural hypothesis.

Mercuric ion resistance levels are readily quantifiable by using an efficiency of plating (EOP) assay, which measures the ability of bacteria to grow on solid media supplemented with $HgCl_2$. The EOP is defined as the ratio of bacteria that survive on plates containing $HgCl_2$ divided by the total number of viable cells that were applied to the plate (Ni'Bhriain et

Table I: Efficiency of Plating Ratios[a] for *E. coli* JM109 Carrying Wild-Type and Mutant *merA*-Containing Plasmids

| plasmid(s) | mutation(s)[b] | transport[c] | IPTG | EOP |
|---|---|---|---|---|
| pJOE114 | wild type | + | − | 1.0 |
| pMMa558a559 | CCAA | + | − | $3.8 \times 10^{-5}$ |
| pMDM1 | $Cys_{135}Cys_{139}$-$Ala_{140}$ | + | − | $5.9 \times 10^{-4}$ |
| pMDM1, pMDO3P15A | $Cys_{135}Cys_{139}$-$Ala_{140}$, AACC | + | − | $3.0 \times 10^{-5}$ |
| | | + | + | $5.1 \times 10^{-5}$ |
| pMMa558a559, pMDO3P15A | CCAA, AACC | + | − | 0.0080 |
| | | + | + | 0.91 |
| pMDO3P15A | AACC | − | − | 0.049 |
| | | − | + | 0.069 |
| no plasmid | | − | − | $2.3 \times 10^{-3}$ |

[a] The efficiency of plating (EOP) ratio is defined as the number of bacterial cells that survive treatment with Hg(II) divided by the total number of viable cells applied to a given plate. [b] AACC and $Cys_{135}Cys_{139}Ala_{140}$ are mutations involving only the redox-active disulfide; CCAA contains only mutations in the C-terminal cysteine pair. [c] (+) indicates the presence of a functional Hg(II) transport system (*merTP*) in addition to the *merA* gene(s) being tested. (−) indicates that the transport system was not present.

al., 1983; Ross et al., 1989). This assay can be used to distinguish three main categories of $HgCl_2$ resistance phenotypes: *resistant*, *sensitive*, and *supersensitive*. Resistant bacteria contain a wild-type *mer* operon whose structural genes (*merPTAD*) encode a specific uptake system for mercuric ions (MerP and MerT) along with mercuric reductase (MerA). These bacteria exhibit an EOP ratio near 1.0 when grown on plates containing up to 50 $\mu$M $HgCl_2$. Sensitive bacteria are those containing no *mer* genes; i.e., they express neither the transport nor the reductase activity. They display EOP values of $10^{-2}$–$10^{-3}$ when plated under the same conditions (i.e., 50 $\mu$M $HgCl_2$). In contrast, bacteria that are supersensitive retain the ability to uptake mercuric ions (*merPT*$^+$) but either lack or have a substantially less active (at least 100-fold for the mutants described here) mercuric reductase (*merA*$^-$). Since these bacteria readily transport Hg(II) into their cytoplasms but are unable to detoxify it by enzymatic reduction, they are more severely affected by mercuric ions than are the sensitive bacteria, which take up Hg(II) only by passive diffusion. This difference translates into EOP ratios for supersensitive bacteria in the range of $10^{-4}$–$10^{-5}$ when grown on 50 $\mu$M $HgCl_2$. By capitalizing on this unique supersensitive phenotype, analysis of EOP ratios can provide an extremely sensitive means to probe mercuric reductase activity in vivo.

In order to express two mutant mercuric reductases in vivo in the same bacterium, we have employed a two-plasmid system in which each mutant gene was placed on a separate plasmid possessing a distinct bacterial origin of replication (ColE1 or P15A) and antibiotic resistance marker (kan$^R$ or amp$^R$). One plasmid also always carried the other *mer* genes in order to provide a fully functional transport system. Additionally, all experiments were performed in the *recA*$^-$ strain, *E. coli* JM109, to eliminate the possibility of homologous recombination when two mutant *merA* genes were present in the host strain concurrently. The plasmids used are schematized in Figure 3A,B.

Table I tabulates the EOP ratios at 50 $\mu$M $HgCl_2$ for a variety of mutant *merA* genes expressed in a transport-positive, *E. coli* JM109 background. Bacteria harboring the plasmid containing wild-type mercuric reductase (pJOE114) exhibited an EOP of 1.0, indicating that these cells are completely resistant to the toxic effects of Hg(II) at that concentration. In contrast, growth of cells containing either pMMa558a559 or pMDM1, which encode the CCAA and AACC mutant

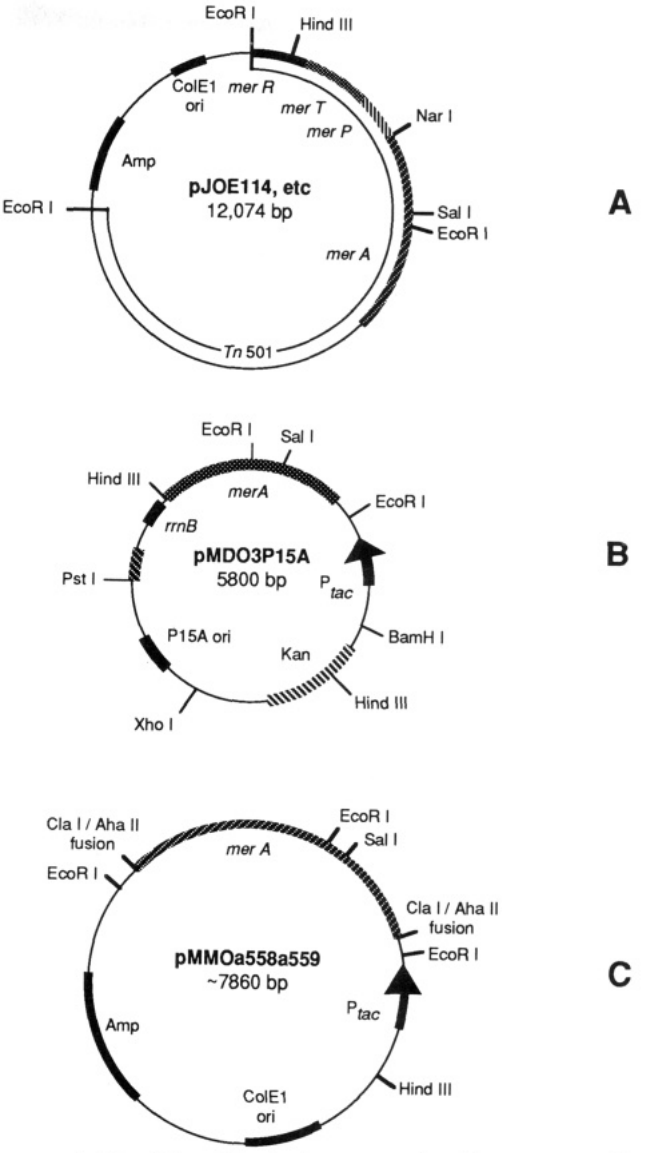


FIGURE 3: Plasmids used for in vivo coexpression of mutant mercuric reductases. Plasmids used in EOP assays were of the types (A) and (B). Plasmid pJOE114 (A) carries wild-type *merA* along with the entire *mer* operon from Tn*501*. Plasmids pMMa558a559 and pMDM1, which were also used in the EOP experiments, are identical with pJOE114 except that they carry the CCAA (pMMa558a559) or $Cys_{135}Cys_{139}Ala_{140}$ (pMDM1) mutations in *merA*. Plasmid pMDO3P15A (B), which was used to express the AACC mutant *merA* gene in trans, contains only *merA* without the remainder of the *mer* operon. This plasmid carries the AACC mutant *merA* gene under control of a *tac* promoter and can coexist in vivo with the above plasmids since it possesses a compatible origin of replication, P15A, along with a different selectable antibiotic resistance marker for kanamycin. The plasmids used for in vivo coexpression of mutant mercuric reductases and for subsequent purification were of the types (B) and (C). The AACC mutant protein was purified from *E. coli* JM109 carrying pMDO3P15A (B). The CCAA mutant protein was purified from *E. coli* JM109 carrying pMMOa558a559 (C). Plasmid pMMOa558a559 (C) positions the CCAA mutant *merA* gene under the control of a *tac* promoter, replicates under the control of the ColE1 origin, and possesses an ampicillin resistance selectable marker. Mercuric reductase heterodimers containing the AACC and CCAA mutants were purified from *E. coli* JM109 carrying pMDO3P15A and pMMOa558a559.

MerAs, respectively, was severely inhibited by Hg(II), with EOP values in the supersensitive range of $10^{-4}$–$10^{-5}$. These results are consistent with previous in vitro studies showing both these mutant proteins to have strongly attenuated catalytic Hg(II) reduction rates (Distefano et al., 1989; Moore & Walsh, 1989). Similar EOP values were obtained in a control

experiment where two redox-active disulfide mutants (AACC *merA* carried on pMDO3P15A and $Cys_{135}Cys_{139}Ala_{140}$ *merA* on pMDM1) were coexpressed in the same bacterium. As expected for different mutations in the same residues, this combination does not provide complementation, but results in EOP values still in the range of $10^{-5}$.

Strikingly different results were obtained when the CCAA and AACC mutant MerAs were coexpressed in cells doubly transformed with pMMa558a559 and pMDO3P15A, respectively. In this case, significant complementation does occur, resulting in EOP values approaching unity (0.91). With this pair of plasmids, it is also interesting to note the effects of IPTG on the EOP values. In the absence of IPTG, an EOP of 0.0080 was obtained. This value is ca. 100-fold higher than that for the constructs described above showing no complementation. Since the AACC mutant *merA* gene present on pMDO3P15A is under control of the *tac* promoter, this low but detectable amount of complementation must result from the "leakiness" of the *tac* promoter in the absence of inducer. When expression of the AACC mutant *merA* gene was further induced by the addition of IPTG in the media, near-wild-type resistance was reached. Thus, the complementation assays with the CCAA and AACC mutants provided the first concrete evidence that the active site of mercuric reductase is comprised of a redox-active disulfide from one subunit and a C-terminal cysteine pair from the other subunit (i.e., an intersubunit active site).

EOP experiments were also performed at 10 and 20 $\mu$M $HgCl_2$ using the same combinations of plasmids as above (data not shown). The measurements performed at 20 $\mu$M $HgCl_2$ were qualitatively similar to those observed with 50 $\mu$M $HgCl_2$, however, the differences between resistant cells and supersensitive cells were much smaller. At 10 $\mu$M $HgCl_2$, no significant sensitivity to mercuric ions was observed with any of the bacteria tested.

*Catalytic Properties of in Vivo Generated Homo- and Heterodimeric Mutant Mercuric Reductases.* To investigate the intersubunit nature of the active site of mercuric reductase in further detail, we next examined the enzymatic activities of several mutant proteins expressed in *E. coli* either individually or together with another mutant. All proteins were expressed in JM109 under control of the *tac* promoter. To express both the CCAA and AACC mutant *merA* genes within the same cell, another two-plasmid system was devised. In this system, plasmid pMMOa558a559 encoded the CCAA mutant while plasmid pMDO3P15A contained the AACC mutant *merA* gene. As described above, the latter plasmid possesses a P15A origin of replication and kanamycin resistance marker. The P15A origin permits the stable maintenance of both mutant plasmids within the same host cell, while the kanamycin resistance element provides a distinct selectable marker for this plasmid. The plasmids used for expression of the various mutant proteins are shown in Figure 3B,C. It should be noted that pMMOa558a559 (Figure 3C) is different from pMMa558a559 and others used in the phenotypic experiments described above in that it contains *only* the *merA* gene of interest and not the *mer* transport genes.

Mutant mercuric reductases were purified by use of Orange A affinity chromatography (Fox & Walsh, 1982). Each protein sample was assayed for mercuric reductase activity as well as NADPH/thioNADP$^+$ transhydrogenase activity (Schultz et al., 1985). The transhydrogenation reaction, which is catalyzed by all mercuric reductase mutants studied to date, is a useful assay for following the purification of mutants that possess very low levels of mercuric reductase activity. The results of these measurements are summarized in Table II. Perusal of these data shows that when mercuric reductases carrying mutations in either the redox-active disulfide (AACC) or the C-terminal cysteine pair (CCAA) are expressed individually, the purified proteins catalyze mercuric ion reduction at less than 1% of the rate of the wild-type enzyme. However, when such mutants are *coexpressed* within the same cell in vivo, the resulting purified protein reduces Hg(II) at 24% of the wild-type rate. A Hanes plot of kinetic data for the coexpressed protein mixture gives a $K_m$ for Hg(II) of 20 $\mu$M which is comparable to the value of 12 $\mu$M observed for the wild-type enzyme (Fox & Walsh, 1982). The relatively high levels of Hg(II) reduction observed only with the purified coexpressed protein again support the hypothesis that the active site of mercuric reductase resides at the subunit interface in the native dimer and that an active site consists of a redox-active disulfide from one subunit and the C-terminal cysteines from the other subunit.

Table II: Catalytic Parameters for Transhydrogenation and Mercuric Ion Reduction Reactions Catalyzed by Purified Wild-Type and Mutant Mercuric Reductases

| plasmid source(s) | mutation(s) | trans-hydrogen-ation (units/mg)[a] | mercuric ion reduction | |
|---|---|---|---|---|
| | | | units/mg[b] | % relative to wild type |
| pPSO1 | wild type | 0.960 | 5.81 | 100 |
| pMDO3P15A | AACC | 5.44 | 0.00693 | 0.12 |
| pMMOa558-a559 | CCAA | 1.94 | 0.0495 | 0.85 |
| pMDO3P15A, pMMOa558-a559[c] | AACC, CCAA | 4.45 | 1.38 | 24 |

[a] One unit of transhydrogenation activity is defined as the thio-NADP$^+$-dependent oxidation of 1 $\mu$mol of NADPH per minute. [b] One unit of mercuric ion reduction activity is defined as the Hg(II)-dependent oxidation of 1 $\mu$mol of NADPH per minute. [c] It should be noted that this purified mercuric reductase sample is a statistical mixture of homodimers and heterodimers.

The crystal structure of human erythrocyte glutathione reductase reveals that the protein dimer has a $C_2$ symmetry axis and thus possesses two identical intersubunit active sites per dimer (Thieme et al., 1981). If mercuric reductase is similarly disposed and the two active sites are equally active, an equimolar ratio of each mutant protein coexpressed in vivo should result in a statistical distribution of 50% homodimers and 50% heterodimers with the heterodimers, in turn, being only 50% active due to the integrity of only one active site per dimer. Such a model predicts the theoretical activity for the purified protein mixture to be 25% that of wild type; the above experimentally determined value was 24%. Although these values are in good agreement, several reasons exist why these numbers need not be equal. First, it should be noted that the mutant genes are expressed on different plasmids; any differences in plasmid copy number, differential gene expression, or differential protein stability may result in a deviation from equimolarity. Additionally, the two putative active sites of the wild-type enzyme are not necessarily identical (Miller et al., unpublished data) and may therefore not contribute equally to enzyme activity. While the latter question regarding the equivalence of active sites cannot be readily addressed by the present experiments, it was possible to assess the relative concentrations of the two mutant proteins within the heterodimeric mixture by two methodologies discussed below.

*Estimation of the Relative Copy Numbers of pMMOa558a559 and pMDO3P15A in E. coli JM109 Harboring Both Plasmids.* Plasmid DNA was isolated from a

culture of *E. coli* JM109 carrying both pMMOa558a559 and pMDO3P15A and analyzed for relative copy numbers as described under Methods. In this way, the ratio of pMMOa558a559 to pMDO3P15A was estimated to be 4.3, meaning that the copy number of pMMOa558a559 is 4.3 times that of pMDO3P15A in cells containing both plasmids. If this ratio accurately reflected the concentration of each mutant translated into protein, the concentration of mutant heterodimers would be 31% of the total mercuric reductase dimers. If then each heterodimer was 50% active (equal active sites), the theoretical activity would be 16% of wild type, instead of the observed value of 24%.

Two points should be noted regarding this manner of estimation of the heterodimeric protein content. First, while this method does give a good indication of the relative plasmid copy number, it may be less accurate in estimating actual protein levels. Although both mutant proteins were overexpressed using the *tac* promoter, the spacing between the promoter and the start of translation was not the same for both mutant genes, and this spacing is known to be particularly important in determining the level of gene expression (Roberts et al., 1979). A second point concerns the bacterial sample from which the plasmid DNA was isolated. It has been found that the number of plasmid molecules per cell increases as the growth rate decreases (Engberg & Nordstrom, 1975); thus, the plasmid copy number within a cell is not constant. The relative copy number above was determined from cells after 5 h of induction with IPTG, i.e., just prior to harvesting for protein purification. Thus, the copy number determined may not necessarily reflect the plasmid copy number present throughout the induction period when protein synthesis was occurring.

*Estimation of the Relative Protein Concentrations of CCAA and AACC Coexpressed in E. coli JM109.* The relative concentrations of CCAA and AACC active sites in the coexpressed mixture of the two proteins were estimated by curve fitting the UV/vis spectrum of the mixture (Figure 4B) to a linear combination of the individual mutant protein spectra (Figure 4A). This method takes advantage of the characteristic spectral differences exhibited by FAD when bound to each mutant protein. However, the validity of this analysis hinges on two suppositions. First, it is necessary to assume that the spectral contributions from both active sites in each homodimeric protein are identical (i.e., identical active sites). Thus, in the coexpressed mixture, only three species are assumed to contribute to the composite spectrum. Two of these are the AACC and CCAA homodimers, both of which are spectroscopically well characterized. The third species is the AACC/CCAA heterodimer which should possess one wild-type active site ($Cys_{135}Cys_{140}$ and $Cys_{558}Cys_{559}$) and one completely mutant active site ($Ala_{135}Ala_{140}$ and $Ala_{558}Ala_{559}$) (Figure 2, bottom). The second assumption inherent in the experiment is that these active sites are spectrally similar to the CCAA and AACC active sites, respectively. In the former case, this is known to be true since the wild-type active site (CCCC) is spectrally indistinguishable from that of CCAA (Moore & Walsh, 1989). That the converse assumption [i.e., an active site containing $Ala_{135}Ala_{140}$ and $Ala_{558}Ala_{559}$ (formally an AAAA mutant) is spectrally identical with an AACC active site] is also valid can be inferred from the spectral properties of other redox-active disulfide mutant proteins. In a comparison of the spectra of the AACC, CACC, and CAAA mutants using second-derivative UV/vis spectroscopy, no differences between these three mutant enzymes were detected (Distefano, 1989). Therefore, it could be concluded that the presence or absence of the C-terminal cysteine residues does not affect the absorbance spectrum of enzyme-bound FAD to any significant extent.

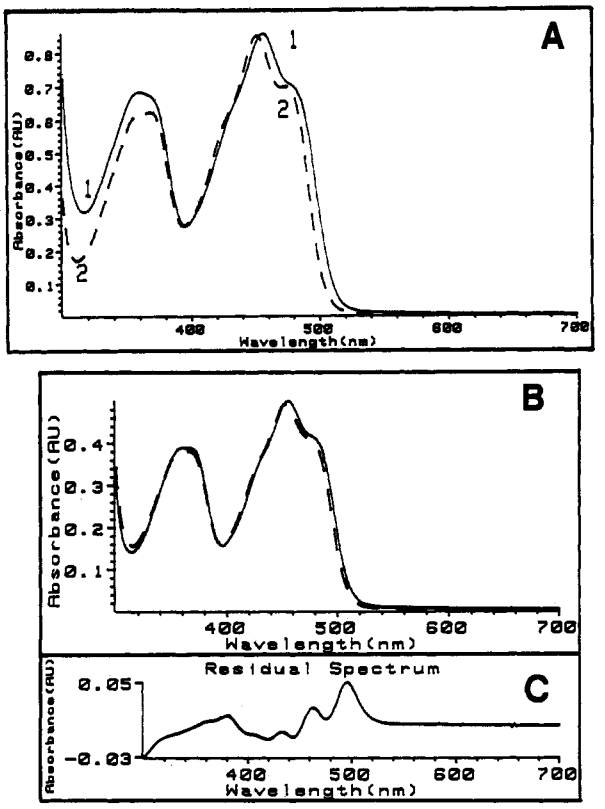


FIGURE 4: Estimation of the concentrations of AACC and CCAA active sites within a heterodimeric mixture using UV/vis spectrophotometry. (A) UV/vis spectra of the purified CCAA (spectrum 1) and AACC (spectrum 2) at equal concentrations (76 μM). (B) Spectra of the purified heterodimeric mixture (solid line) and "best fit" spectrum (dashed line) composed of a linear combination of the two spectra shown in (A). (C) Residual difference spectrum obtained by subtracting the "best fit" computed spectrum from the actual spectrum of the purified heterodimeric mixture shown in (B).

The observed spectrum of the coexpressed AACC/CCAA protein mixture and the best-fit spectrum derived via the curve-fitting program are presented in Figure 4B. The residual difference spectrum between these two is shown Figure 4C. This analysis gave values of 16.2 μM for the concentration of AACC and 27.5 μM for [CCAA]. Therefore, the ratio of CCAA to AACC active sites was 1.70, generating a population of heterodimers that would comprise 47% of the total mixture of homodimers and heterodimers. Such a mixture would be expected to display 24% of the specific activity of wild type, identical with the experimentally determined value.

*In Vitro Heterodimer Formation between Purified AACC and CCAA Mutant Enzymes Using Chaotropic Agents.* In addition to the in vivo experiments presented above, in vitro mixing experiments were also performed starting with pure AACC and pure CCAA homodimers. Initially, the chaotropic agents KSCN, $NaClO_4$, and guanidine hydrochloride were screened for their ability to promote MerA subunit interchange in samples containing equimolar amounts of the two inactive mutant proteins. In these experiments, the protein mixtures were dialyzed against each chaotrope dissolved in buffer, with dialysates containing no chaotrope and similarly treated wild-type samples serving as controls. After 120 h at 4 °C, all the enzyme samples (except that dialyzed against buffer alone) had become completely bleached, i.e., the flavin had been effectively removed. Samples were renatured in excess FAD, desalted by gel filtration, and assayed for mercuric reductase activity. The results are summarized in Table III.

Table III: Relative Activities of Wild-Type and AACC/CCAA[a] after Exhaustive Dialysis against Chaotropic Agents

| enzyme | chaotrope | relative activity[b] |
|---|---|---|
| wild type | none | 100 |
| | 1.5 M KSCN | 86 |
| | 1.5 M $NaClO_4$ | 117 |
| | 1 M guanidine hydrochloride | 102 |
| AACC/CCAA | none | −3.1[c] |
| | 1.5 M KSCN | 15.8 |
| | 1.5 M $NaClO_4$ | 21.2 |
| | 1 M guanidine hydrochloride | 21.1 |

[a] An equimolar mixture of CCAA and AACC. [b] Calculated by determining the activity level in 100 μM $HgCl_2$, 2 mM β-mercaptoethanol, and 200 μM NADPH and then normalizing for protein concentration. Activity levels were taken as the Hg(II)-stimulated NADPH oxidation rate minus the Hg(II)-independent NADPH oxidation rate. [c] AACC has a very high inherent oxidase rate (ca. 23 $min^{-1}$) which is inhibited by mercurials (Distefano et al., 1989; Distefano, 1989). This explains the negative value here.

Several key points emerged from the above experiments. First, prolonged exposure to the chaotropic agents had little effect on wild-type activity (i.e., there was no irreversible denaturation of the enzyme). Second, no increase in activity was seen for the 1:1 CCAA/AACC homodimer mixture when dialyzed against buffer alone. Thus, in the absence of chaotropes, mercuric reductase dimers must be extremely stable ($t_{1/2}$ for interchange ≫120 h at 4 °C). Finally, all three CCAA/AACC samples that had been exposed to chaotropic reagents showed significantly increased activity levels. In fact, their activities approached the theoretical maximum of 25% wild-type activity. Therefore, like the findings with protein mixtures generated in vivo, these results strongly support the assertion that the active site of mercuric reductase is composed of cysteine residues from both subunits.

To examine the time course of subunit mixing, small samples containing CCAA and AACC homodimers were made 1.5 M in either KSCN or guanidine hydrochloride, and at selected intervals, aliquots were withdrawn and assayed as above. These experiments indicated that 1.5 M KSCN promotes subunit hybridization relatively quickly, with 120 min being sufficient for >90% of the increase in activity occur. In contrast, the changes in activity levels brought on by 1.5 M guanidine hydrochloride plateaued at half those of KSCN after only 60 min (data not shown). [Only after prolonged incubation with the enzyme (vide supra) did guanidine hydrochloride yield activity levels near those generated by KSCN.] The optimal concentration of KSCN was determined similarly except that [KSCN] was varied from 0.0 to 1.5 M while hybridization time was held constant at 120 min. This experiment demonstrated that either 1.4 or 1.5 M KSCN promoted the highest increase in activity after 2 h (data not shown).

*Electrophoretic Separation of a Heterodimeric Mixture Prepared in Vitro from "Clipped" AACC and "Unclipped" CCAA: Evidence for a Heterodimeric Species of Intermediate Mobility.* In both the in vivo and in vitro experiments described above, an increase in mercuric reductase activity could be correlated with the coexpression or mixing of two inactive mutant proteins. Yet, while these results strongly implied the formation of active heterodimers from inactive homodimers, no explicit proof of this conclusion could be obtained because the putative heterodimeric species did not possess inherently distinctive properties that allowed its separation from the homodimers. However, the ability to prepare heterodimers in vitro made it possible to proteolytically modify one mutant protein prior to heterodimer formation. Fox and Walsh (1983) had previously shown that the N-terminal 85 amino acids can be removed ("clipped") from wild-type mercuric reductase without affecting its catalytic activity. Thus, when heterodimers are prepared in vitro from one partially proteolyzed ("clipped") mutant (subunit molecular mass of 50 kDa) and one intact ("unclipped") mutant (subunit molecular mass of 59 kDa), the resulting heterodimers should consist of one clipped and one unclipped subunit. Since partial proteolysis removes a relatively large polypeptide segment (85 out of 561 residues), it was anticipated that nondenaturing gel electrophoresis would allow unclipped homodimers (118-kDa dimer), heterodimers (109-kDa dimer), and clipped homodimers (100-kDa dimer) to be separated as species of increasing electrophoretic mobility.

An SDS–PAGE separation of clipped AACC and freshly isolated, unclipped CCAA homodimers is shown in Figure 5A. While the clipped sample is homogeneous, the unclipped sample clearly contains several partial proteolytic products; this occurs despite the isolation of this protein in buffer containing the protease inhibitor, PMSF. Nonetheless, this sample consists predominantly and usably of the unclipped form. Figure 5B (lanes 2 and 3) shows 30 μg of these same samples electrophoresed on a nondenaturing polyacrylamide gel, where they again clearly exhibit *different* electrophoretic mobilities. Additionally, electrophoresis of a sample containing both proteins combined in the absence of chaotrope (Figure 5B, lane 4) shows that the native species can also be cleanly resolved from a mixture of homodimers. The key result is shown in lane 5. This lane contains the same sample as in lane 4 except that in this case it was treated with the chaotropic agent, KSCN, and desalted prior to electrophoresis. As is indicated by the arrows, two new electrophoretically distinct species appear upon such treatment. Since the unclipped sample of CCAA (Figure 5A, lane 2) contains at least two species having differential electrophoretic mobilities, it is not unreasonable that one should observe two new species upon treatment of the AACC/CCAA mixture with KSCN. In Figure 5C, a bar graph is shown depicting the amount of mercuric reductase activity loaded onto each lane of the native gel in Figure 5B. As can be readily seen, the only lane with a significant level of activity is that which contains the sample treated with the chaotropic agent; this is also the lane which contains the two new protein bands.

In order to identify the two new species that appeared in the native gel after chaotropic treatment of the clipped AACC and unclipped CCAA enzyme mixture, individual bands were excised from a preparative native gel, eluted, and examined by SDS–PAGE (Figure 5D). From this analysis, it is clear that the new protein bands do contain both clipped and unclipped proteins. Thus, the new bands must be heterodimeric species, resulting from the combination of monomers of the different size mutant proteins. In aggregate, the data presented in Figure 5A–D clearly revealed detection of discrete, active heterodimeric mercuric reductase enzyme species.

## Discussion

This paper has described in vivo and in vitro experiments in which active heterodimers of mercuric reductase were formed from bis(cysteine), bis(alanine) mutant proteins that are inactive when present as homodimers. Two different methodologies were employed to generate the heterodimers. First, an active heterodimeric enzyme mixture was formed in vivo by coexpression of the two inactive mutant genes in the same bacterium. By formation of the heterodimers in vivo, the natural efficiency of subunit assembly which occurs in the cytoplasmic environment can be used to an advantage. Such

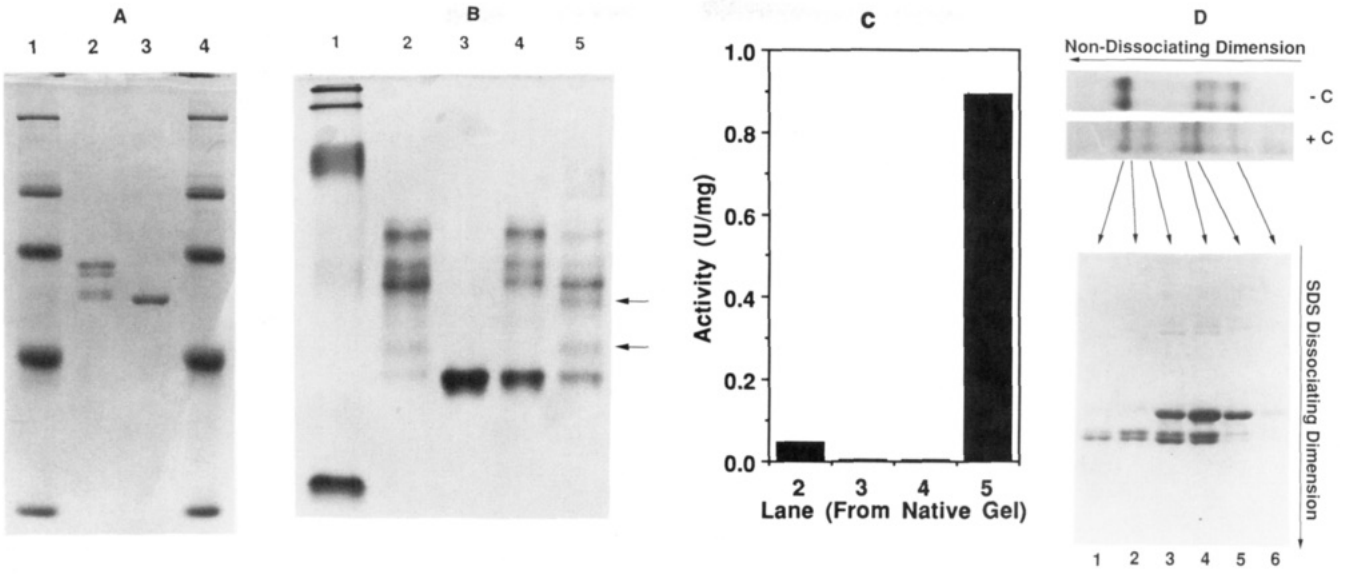


FIGURE 5: (A) SDS–PAGE analysis of freshly isolated "unclipped" CCAA and "clipped" AACC. (Lane 1) Molecular mass standards: myosin, 200 kDa; phosphorylase *b*, 97 kDa; bovine serum albumin, 68 kDa; ovalbumin, 43 kDa; carbonic anhydrase, 29 kDa. (Lane 2) Freshly isolated, predominantly unclipped CCAA protein. (Lane 3) Clipped AACC obtained by limited proteolysis with chymotrypsin followed by Orange A affinity chromatography. (Lane 4) Molecular mass standards as in lane 1. (B) Separation by native PAGE of heterodimeric mercuric reductase prepared from "clipped" AACC and "unclipped" CCAA. (Lane 1) Molecular mass standards: thyroglobin, 670 kDa; ferritin, 440 kDa; catalase, 230 kDa; aldolase, 160 kDa; bovine serum albumin, 68 kDa. Note that aldolase is only faintly detectable, migrating near the most intense band in lane 2. (Lane 2) 30 $\mu$g of freshly prepared, predominantly unclipped CCAA. (Lane 3) 30 $\mu$g of clipped AACC. (Lane 4) A mixture of 15 $\mu$g of predominantly unclipped CCAA and 15 $\mu$g of clipped AACC in the absence of chaotrope. (Lane 5) A sample identical with that in lane 4 except treated with 1.5 M KSCN for 3 h and then desalted (NAP-10, Pharmacia) prior to loading. The arrows indicate two new bands that appear in lane 5 which are not present in lane 4. (C) Specific activities of homodimeric and heterodimeric samples fractionated by nondissociating PAGE. Prior to electrophoretic separation (Figure 5B), the mercuric reductase activity of each sample was determined. As shown in this graph, only lane 5, which contains both the AACC and CCAA mutant proteins which have been treated with the chaotrope, KSCN, shows significant activity. (D) Two-dimensional electrophoretic analysis of a heterodimeric mixture prepared from clipped AACC and unclipped CCAA. A nondissociating gel was used to separate mixtures of clipped AACC and predominantly unclipped CCAA (top). (+C) and (–C) denote whether the sample was or was not treated, respectively, with chaotrope prior to gel loading. Protein bands corresponding to the (+C) lane were excised and eluted and then analyzed by SDS–PAGE (bottom) as described under Methods. Note that the two new bands that appeared in the (+C) lane of the native gel contain both unclipped and clipped monomers.

methodology may be of particular importance in the manipulation of species possessing complex metal centers or cofactors which can be irreversibly disrupted by using conventional in vitro mixing techniques. In the latter portion of this paper, heterodimers were formed in vitro. With this method, it is possible to manipulate, and hence effectively "tag", one of the mutant proteins prior to heterodimer formation. Such pretreatment can give rise to a heterodimer with properties intermediate between those of the modified and unmodified homodimers, allowing separation and specific characterization of the heterodimers [see Wente and Schachman (1987) for an example].

Two types of in vivo experiments were described. In both cases, heterodimers were formed by using an expression system where each mutant *merA* gene was placed on a separate plasmid having a distinct origin of replication. In the first set of experiments, one plasmid also encoded the remainder of the *mer* operon (transport genes etc.), allowing the effect of heterodimer formation on mercury resistance levels to be examined. These experiments demonstrated that coexpression of inactive redox-active disulfide (AACC) and C-terminal cysteine (CCAA) mutants in vivo resulted in a ca. 1000-fold increase in the level of resistance to $HgCl_2$ when compared with bacteria harboring only one of the mutant genes. This was determined by using an efficiency of plating (EOP) assay (Ni'Bhriain et al., 1983; Ross et al., 1989), where the EOP is defined as the number of bacteria that survive on plates containing $HgCl_2$ divided by the total number of viable cells applied to the plate.

As a biochemical complement to the phenotypic experiments, the enzymatic activity of heterodimers produced in vivo was assessed by using a protein sample purified from bacteria expressing both mutant proteins under control of the *tac* promoter. The specific activity of this AACC/CCAA sample was 24% that of wild-type mercuric reductase, in good agreement with the theoretical value of 25% activity expected from a heterodimeric mixture formed from equimolar ratios of each mutant protein. Two methods were used to quantitate the actual relative concentrations of the two proteins. The first, in which the copy number ratio of the two plasmids was assessed, indicated that one plasmid was present over the other in a 4.3 to 1 excess. However, spectral quantitation of the purified heterodimeric protein mixture suggested that the two mutants are present in a ratio closer to unity (1.7:1), and this protein ratio would be expected to yield the same level of enzyme activity as was experimentally observed.

In regard to the in vivo generation of active heterodimers from inactive mutants, it is worth noting the novel nature of the phenotypic experiments described here. In this context, Larimer et al. (1987) have previously described a two-plasmid system similar to the one we used to determine the specific activity of the purified heterodimeric mixture. However, our phenotypic complementation experiments took advantage of the fact that a functional mercuric reductase confers an enormous phenotypic difference (quantifiable by the EOP assay) upon bacteria expressing a functional Hg(II) transport system when compared to similar bacteria expressing an inactive mercuric reductase. *Thus, by simply counting bacterial colonies on petri plates, important information about the location of catalytic residues within the active site of this enzyme can be obtained.*

Active, heterodimeric mercuric reductases were also ob-

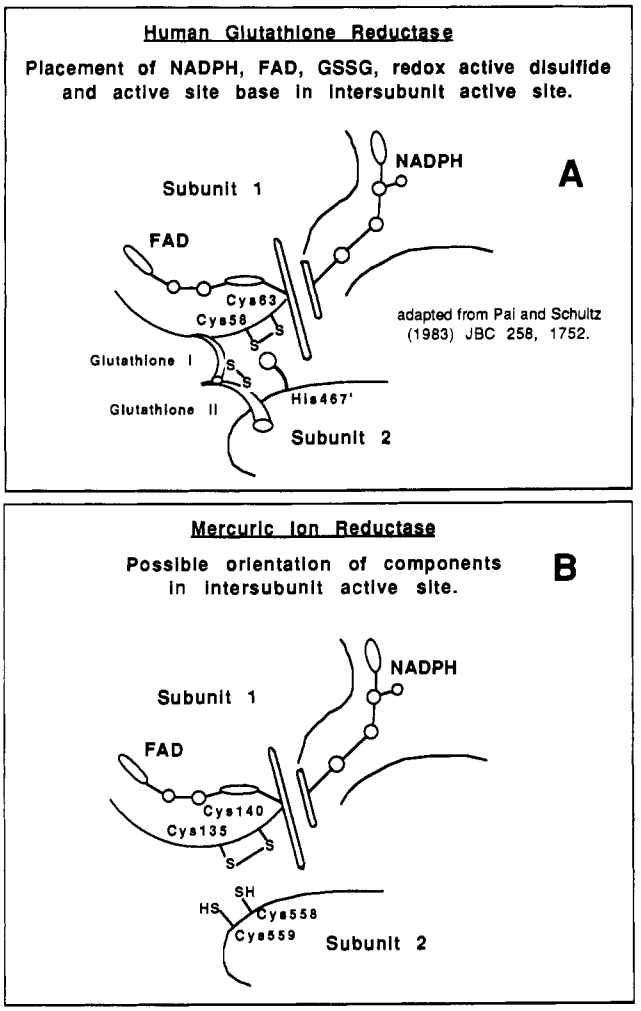


FIGURE 6: Schematic views of the glutathione reductase and possible mercuric reductase active sites. (A) Schematic active site of human glutathione reductase showing the redox-active disulfide ($Cys_{58}$ and $Cys_{63}$) and the active-site base, $His_{467}$. (B) Possible active-site structure of mercuric reductase showing the redox-active disulfide ($Cys_{135}$ and $Cys_{140}$) from one subunit and the C-terminal cysteine pair ($Cys_{558}$ and $Cys_{559}$) from the opposite subunit.

tained by mixing the inactive AACC and CCAA mutant proteins in the presence of chaotropic agents in vitro. To provide physical evidence that heterodimers were really formed in these experiments, in vitro mixing was performed using the "unclipped" form of one mutant and the "clipped" form (obtained through limited chymotryptic digestion) of the other mutant. Nondissociating PAGE of such mutants indicated that the partially proteolyzed homodimers were clearly separable from unmodified homodimers. Treatment of a mixture of the two mutants with KSCN resulted in the formation of two new species with electrophoretic mobilities intermediate between those of the parent homodimers. SDS–PAGE revealed that these two new species contained both clipped and unclipped monomers, showing that mixing of the two mutants in the presence of chaotropic agents does indeed result in heterodimer formation.

Taken together, the experimental data presented here provide compelling evidence that the active site in mercuric reductase resides at the interface between subunits and that it is made up of a redox-active disulfide from one subunit and a C-terminal cysteine pair from the adjacent subunit. Such an arrangement compares favorably with the very similar enzyme glutathione reductase. Figure 6A shows a cartoon diagram which summarizes many of the salient features of the glutathione reductase 2.0-Å crystal structure (Pai & Schulz, 1983). Shown in this figure is the intersubunit nature of the active site as well as the participation of the redox-active disulfide ($Cys_{58}$ and $Cys_{63}$) from one subunit and $His_{467}$ from the opposite subunit. Figure 6B shows a similar possible active-site configuration for mercuric reductase. Particularly important in this diagram is the clustering of the redox-active cysteines ($Cys_{135}$ and $Cys_{140}$) and C-terminal cysteines ($Cys_{558}$ and $Cys_{559}$) from distinct subunits to form a competent active site. Future experiments that address the mechanism of Hg(II) reduction catalyzed by mercuric reductase must take into account and examine this four-cysteine, intersubunit active site.

## ACKNOWLEDGMENTS

We thank Dr. Anne Summers, University of Georgia, for advice with the in vivo efficiency of plating experiments and Dr. Stan Tabor for advice concerning the pGP1-4 vector.

**Registry No.** L-Cys, 52-90-4; mercuric reductase, 67880-93-7.

## REFERENCES

Beinert, H., Orme-Johnson, W. H., & Palmer, G. (1978) *Methods Enzymol. 64*, 111.

Bradford, M. M. (1976) *Anal. Biochem. 72*, 248.

Brown, N., Ford, S., Pridmore, R., & Fritzinger, D. (1983) *Biochemistry 22*, 4089.

Davis, B. J. (1964) *Ann. N.Y. Acad. Sci. 121*, 404.

Distefano, M. D. (1989) Ph.D. Thesis, Department of Chemistry, Massachusetts Institute of Technology.

Distefano, M. D., Au, K. A., & Walsh, C. T. (1989) *Biochemistry 28*, 1168.

Engberg, B., & Nordstrom, K. (1975) *J. Bacteriol. 123*, 179.

Fincham, J. R. S., & Coddington, J. (1963) *J. Mol. Biol. 6*, 361.

Fox, B., & Walsh, C. (1982) *J. Biol. Chem. 257*, 2498.

Fox, B., & Walsh, C. (1983) *Biochemistry 22*, 4082.

Garen, A., & Garen, S. (1963) *J. Mol. Biol. 7*, 13.

Griffin, H., Foster, T., Silver, S., & Misra, T. (1987) *Proc. Natl. Acad. Sci. U.S.A. 84*, 3112.

Hatefi, Y., & Hanstein, W. G. (1974) *Methods Enzymol. 31*, 770.

Hewlett Packard (1987) *HP89500 UV/VIS ChemStation Quantitation Software Handbook*, Publication No. 89511-90001, Jan 1987, Hewlett Packard, Palo Alto, CA.

Jaenicke, J. R., & Rudolf, R. (1986) *Methods Enzymol. 131*, 218.

Krauth-Siegel, R. L., Blatterspiel, R., Saleh, M., Schiltz, E., Schirmer, R. H., & Untucht-Grau, R. (1982) *Eur. J. Biochem. 121*, 259.

Larimer, F. W., Lee, E. H., Mural, R. J., Soper, T. S., & Hartman, F. C. (1987) *J. Biol. Chem. 262*, 15327.

Lowry, O. H., Rosebrough, N. J., Farr, A. L., & Randall, R. J. (1951) *J. Biol. Chem. 193*, 265.

Maniatis, T., Fritsch, E. F., & Sambrook, J. (1982) *Molecular Cloning: A Laboratory Manual*, Cold Spring Harbor Laboratory, Cold Spring Harbor, NY.

Miller, S. M., Massey, V., Ballou, D. P., Williams, C. H., & Walsh, C. (1986) *J. Biol. Chem. 261*, 8081.

Miller, S. M., Moore, M., Massey, V., Williams, C. H., Jr., Distefano, M., Ballou, D., & Walsh, C. T. (1989) *Biochemistry 28*, 1194.

Misra, T., Brown, N., Fritzinger, D., Pridmore, R., Barnes, W., Haberstroh, L., & Silver, S. (1984) *Proc. Natl. Acad. Sci. U.S.A. 81*, 5975.

Moore, M. J., & Walsh, C. T. (1989) *Biochemistry 28*, 1183.

Ni'Bhriain, N. N., Silver, S., & Foster, T. J. (1983) *J. Bacteriol. 155*, 690.

Pai, E. F., & Schulz, G. E. (1983) *J. Biol. Chem. 258*, 1752.
Roberts, T. M., Kacich, R., & Ptashne, M. (1979) *Proc. Natl. Acad. Sci. U.S.A. 76*, 5596.
Ross, W., Park, S. J., & Summers, A. O. (1989) *J. Bacteriol. 171*, 4009.
Schlesinger, M. J., & Levinthal, C. (1963) *J. Mol. Biol. 7*, 1.
Schultz, P., Au, K., & Walsh, C. (1985) *Biochemistry 24*, 6840.
Shames, S. L., Fairlamb, A. H., Cerami, A., & Walsh, C. (1986) *Biochemistry 25*, 3519.
Silver, S., & Misra, T. K. (1988) *Annu. Rev. Microbiol. 42*, 717.
Stephens, P. E., Lewis, H. M., Darlison, M. G., & Guest, H. R. (1983) *Eur. J. Biochem. 135*, 519.
Summers, A. O. (1986) *Annu. Rev. Microbiol. 40*, 607.
Thieme, R., Pai, E. F., Schirmer, R. H., & Schulz, G. E. (1981) *J. Mol. Biol. 152*, 763.
Wang, Y., Moore, M., Levinson, H., Silver, S., Walsh, C., & Mahler, I. (1989) *J. Bacteriol. 171*, 83.
Wente, S. R., & Schachman, H. K. (1987) *Proc. Natl. Acad. Sci. U.S.A. 84*, 31.

# Phosphorylation of Bovine Platelet Myosin by Protein Kinase C†

Mitsuo Ikebe* and Sheila Reardon
*Department of Physiology and Biophysics, Case Western Reserve University, Cleveland, Ohio 44106*
*Received June 16, 1989; Revised Manuscript Received October 27, 1989*

ABSTRACT: Bovine platelet myosin is phosphorylated by protein kinase C at multiple sites. Most of the phosphate is incorporated in the 20 000-dalton light chain although some phosphate is incorporated in the heavy chain. Phosphorylation of the 20 000-dalton light chain of platelet myosin is 10 times faster than the phosphorylation of smooth muscle myosin. Platelet myosin light chain is first phosphorylated at a threonine residue followed by a serine residue. Dominant phosphorylation sites of the 20 000-dalton light chain are estimated as serine-1, serine-2, and threonine-9. Prolonged phosphorylation by protein kinase C resulted in an additional phosphorylation site which, on the basis of limited proteolysis, appears to be either serine-19 or threonine-18. Phosphorylation by protein kinase C causes an inhibition of actin-activated ATPase activity of platelet myosin prephosphorylated by myosin light chain kinase. Inhibition of ATPase activity is due to a decreased affinity of myosin for actin, and no change in $V_{max}$ is observed. It is shown that platelet myosin also exhibits the 6S to 10S conformation transition as judged by viscosity and gel filtration methods. $Mg^{2+}$-ATPase activity of platelet myosin is paralleled with the 10S–6S transition. Phosphorylation by protein kinase C affects neither the 10S–6S transition nor the myosin filament formation. Therefore, the inhibition of actin-activated ATPase activity of platelet myosin is not due to the change in the myosin conformation.

The contractile proteins actin and myosin have been found in many eukaryotic cells and are thought to have important roles in cell function. Blood platelets provide a good model system to study the function of nonmuscle actomyosin, since contractile proteins are the dominant proteins of the platelet cytoplasm (Pollard et al., 1977; Korn, 1978).

In platelets as well as in smooth muscle, skeletal muscle, cardiac muscle, and several nonmuscle cells, it has been shown that the light chain of myosin is phosphorylated (Adelstein et al., 1977; Daniel et al., 1981). The significance of this phosphorylation is best understood in the case of smooth muscle myosin which is phosphorylated by a calcium–calmodulin-dependent protein kinase, myosin light chain (MLC)[1] kinase (Hartshorne, 1987). Phosphorylation of the 20 000-Da light chain of myosin has been shown to be a prerequisite for actin-activated ATPase activity of smooth muscle myosin (Hartshorne, 1987).

Platelets also contain a protein kinase that phosphorylates the 20 000-dalton light chain of platelet myosin (Hathaway et al., 1979), and this activates the actomyosin ATPase activity (Adelstein & Conti, 1975). Thrombin induces several platelet responses including shape change, aggregation, secretion, and clot retraction, and it is thought that phosphorylation of the 20 000 dalton light chain of myosin is associated with the activation of platelets. The protein kinase catalyzing this phosphorylation has been identified as myosin light chain kinase (Adelstein et al., 1977; Daniel et al., 1981).

It is known that tumor-promoting phorbol esters can also cause platelet aggregation and phosphorylation of the 20 000-dalton peptide of intact platelets (Chiang et al., 1981; Caroll et al., 1982). Naka et al. (1983) reported that 12-*O*-tetradecanoylphorbol 13-acetate (TPA) induced the phosphorylation of the 20 000-dalton light chain of myosin during the activation of platelets. They also found that the phosphorylation induced by TPA is mediated mainly by protein kinase C but not by myosin light chain kinase.

Recently, it has been shown that protein kinase C phosphorylates the smooth muscle myosin at a single site on a threonine residue (Nishikawa et al., 1984). Subsequently, it was found that three sites can be phosphorylated, and these sites were determined to be threonine-9, serine-1, and serine-2 of the 20 000-dalton light chain (Ikebe et al., 1987a; Bengur et al., 1987). Phosphorylation alone does not affect the enzymatic properties of HMM, although phosphorylation of

† This work was supported by a grant from the American Heart Association Northeast Ohio Affiliate. M.I. is an Established Investigator of the American Heart Association and is a Syntex Scholar.
* Address correspondence to this author.

[1] Abbreviations: MLC, myosin light chain; HMM, heavy meromyosin; HPLC, high-performance liquid chromatography; EGTA, ethylene glycol bis(β-aminoethyl ether)-*N*,*N*,*N*′,*N*′-tetraacetic acid; PMA, phorbol 12-myristate 13-acetate; DTT, dithiothreitol; PMSF, phenylmethanesulfonyl fluoride; HEPES, *N*-(2-hydroxyethyl)-piperazine-*N*′-2-ethanesulfonic acid; SDS, sodium dodecyl sulfate.

0006-2960/90/0429-2713$02.50/0 